Cellular Signalling 58 (2019) 34–43

Contents lists available at ScienceDirect

Cellular Signalling

journal homepage: www.elsevier.com/locate/cellsig

G protein αq exerts expression level-dependent distinct signaling paradigms

Dinesh Kankanamge[a], Mithila Tennakoon[a], Amila Weerasinghe[b], Luis Cedeno-Rosario[c], Deborah N. Chadee[c], Ajith Karunarathne[a,*]

[a] Department of Chemistry and Biochemistry, The University of Toledo, Toledo, OH 43606, USA
[b] McDonnell Genome Institute, Washington University in St. Louis, St. Louis, MO 63108, USA
[c] Department of Biological Sciences, The University of Toledo, Toledo, OH 43606, USA

ARTICLE INFO

Keywords:
GPCR
G protein
Signal transduction
Calcium

ABSTRACT

G protein αq-coupled receptors (Gq-GPCRs) primarily signal through GαqGTP mediated phospholipase Cβ (PLCβ) stimulation and the subsequent hydrolysis of phosphatidylinositol 4, 5 bisphosphate (PIP2). Though Gq-heterotrimer activation results in both GαqGTP and Gβγ, unlike Gi/o-receptors, it is unclear if Gq-coupled receptors employ Gβγ as a major signal transducer. Compared to Gi/o- and Gs-coupled receptors, we observed that most cell types exhibit a limited free Gβγ generation upon Gq-pathway and Gαq/11 heterotrimer activation. We show that cells transfected with Gαq or endogenously expressing more than average-levels of Gαq/11 compared to Gαs and Gαi exhibit a distinct signaling regime primarily characterized by recovery-resistant PIP2 hydrolysis. Interestingly, the elevated Gq-expression is also associated with enhanced free Gβγ generation and signaling. Furthermore, the gene GNAQ, which encodes for Gαq, has recently been identified as a cancer driver gene. We also show that GNAQ is overexpressed in tumor samples of patients with Kidney Chromophobe (KICH) and Kidney renal papillary (KIRP) cell carcinomas in a matched tumor-normal sample analysis, which demonstrates the clinical significance of Gαq expression. Overall, our data indicates that cells usually express low Gαq levels, likely safeguarding cells from excessive calcium as wells as from Gβγ signaling.

1. Introduction

GPCRs primarily control cellular processes by transduction of extracellular information via activating heterotrimeric G proteins [1–4]. With their crucial juncture in cellular signaling, GPCRs-G proteins are implicated in numerous diseases including cancer and heart disease, thus have become the largest drug target. Gαs (stimulatory) and Gαi (inhibitory) members of Gα family are primary regulators of adenylyl cyclase (AC)-cAMP signaling, in directions implied by their names. Based on structural similarities, a third subfamily member, Gq/11 further categorized into Gαq, Gα11, Gα14, and Gα15/16 and regulates several distinct signaling pathways [5–7].

The Gq/11 subfamily plays a pivotal role in cardiac, lung, brain, immune and circulatory functions [8–10]. Activated PLC acts on phosphatidylinositol 4, 5-bisphosphate (PIP2), a membrane phospholipid to generate diacyl glycerol (DAG) and inositol 1, 4, 5-triphosphate (IP3). DAG and IP3 serve as second messengers for PKC activation and intracellular calcium mobilization in cells. PIP2 also plays an important role in membrane trafficking [11–15], cytoskeleton functions [16,17], and ion transporters and channels activation [18–20]. However, both IP3 and DAG are recycled to resynthesize phosphatidylinositol (PtdIns) [21,22], followed by phosphatidylinositol 4-kinase and phosphatidylinositol 4-phosphate mediated sequential phosphorylation to generate PIP2 [23,24]. Minutes after Gq-pathway mediated PIP2 hydrolysis, many cell types show PIP2 recovery despite the presence of the active Gq-pathway. While such a resynthesis is essential in maintaining PIP2, especially against the fast rate of Gq-GPCR mediated PIP2 hydrolysis [21], the regulation of this PIP2 regeneration (recovery) is unclear [21,22]. Specifically, it is not clear if the initial PIP2 hydrolysis triggers this PIP2 recovery process [25–27].

IP3 generated after PIP2 hydrolysis activates IP3 receptors and induces stored calcium release [28,29]. To maintain resting Ca^{2+} concentrations, PM and Sarcoplasmic reticulum Ca^{2+}ATPase pumps remove Ca^{2+} from the cytosol. Therefore, Gq/11 mediated Ca^{2+} homeostasis is important in many cellular functions including skeletal mineralization, muscle contraction, nerve impulse transmission, blood clotting, and hormone secretion [30]. Excessive calcium signaling has been reported in many disease conditions [31–34]. Control of protein kinase C (PKC) by Gq/11 is crucial for activation of essential proteins and lipids that are responsible for cell survival [35]. Excessive PKC

* Corresponding author.
E-mail address: Ajith.karunarathne@utoledo.edu (A. Karunarathne).

https://doi.org/10.1016/j.cellsig.2019.02.006
Received 8 November 2018; Received in revised form 23 February 2019; Accepted 25 February 2019
Available online 05 March 2019

signaling diminishes prefrontal neuronal firing and induces chronic stress [36]. In vitro studies in hippocampal cell cultures exhibited cytoskeleton spine collapse and disruption of the actin cytoskeleton upon elevation of PKC signaling [37]. Excessive PKC activation severely impaired cognitive functions of the prefrontal cortex in rodents and is predicted to be implicated in diabetic cardiomyopathy [38–40]. Elevated PKC signaling can also contribute to diabetic neuropathy, likely through its effects on vascular blood flow [35].

Many biochemical and biophysical studies proved that G protein heterotrimers dissociate into GαGTP and Gβγ [41,42]. We have shown that all Gβγ complexes translocate to IMs upon Gi/o and Gs-coupled GPCR receptor activation, indicating the physical dissociation of the heterotrimer [43]. However, several studies showed evidence for lack of heterotrimer dissociation during activation as well [44–46]. For instance, simple subunit rearrangements over physical dissociation of heterotrimers was demonstrated using resonance energy transfer studies [46,47]. Gi/o and Gs-pathway activation regulate signaling both through Gβγ as well as Gαi-GTP. Gαs and Gαi-GTP regulate adenylyl cyclase (AC) and cAMP. On the contrary, Gβγ generated regulates many effectors including PI3Kγ [48], adenylyl cyclase (AC) isoforms [49,50], PLCβ isoforms [1]. Gβγ is also known to activate Ca^{2+} channels (N, P/Q type) [2,51], inwardly rectifying potassium channels (GIRK) [52,53] and GPCR kinase (GRK2, GRK3) [54]. Several guanine nucleotide exchange factors (GEFs) are also found to be activated by Gβγ such as Rac (FLJ00018), Cdc42 (p114-RhoGEF) [55–57]. Interestingly, compared to Gαi- and Gαs-GPCR activations, in many cell types Gαq-GPCR activation failed to induce a detectable Gβγ translocation [58]. PLCβ activation has been identified as the primary function of the Gq-pathway [5,6,8,59], but the lack of evidence for Gβγ signaling suggests that Gq-pathway activation generates only a limited number of heterotrimers. Either lack of physical dissociation of Gq-heterotrimers, lower expression of Gαq or fast GTP hydrolysis on Gαq-GTP can prevent Gβγ translocation. Recent identification of the Gαq/11 subfamily as major cancer driver genes signify the importance of understanding Gq-pathway regulation [60,61]. Here, we examined repercussions of differential Gαq expression levels on signaling outcomes in cells to decipher why cells may require tight regulation of Gq/11 pathway signaling.

2. Materials and methods

2.1. DNA constructs, reagents and cell lines

cDNAs; M3R and YFP-PH, have been previously discussed [62,63]. The constructs; α2-AR, mCherry-γ9, GFP-γ9, αq-CFP, YFP-γ1, 11 and β1-YFP were kindly provided by Professor N. Gautam, Washington University, St. Louis, MO. GRPR and PKCδ-GFP were kindly gifted by Dr. Zhou-Feng Chen's lab, Washington University, St. Louis, MO. GRK2 and Opn4 were previously described [64]. Opn4-YFP was created by PCR amplification of Opn4 with *Kpn*I and *Xba*I from Opn4 untagged and subcloned to corresponding restriction sites generated after restriction digestion of GRK2-YFP. Reagent sources are as follows: Norepinephrine and PTx (SigmAldrich, St. Louis, MO, USA), YM-254890 (Focus Biomolecules, Plymouth Meeting, PA, USA), Bombesin (Tocris, Park Ellisville, MO, USA), Carbachol (Fisher Scientific, Pittsburgh, PA, USA), SDF-1α (PeproTech, Rocky Hill, NJ, USA), Lipofectamine 2000 and Gallein (Thermo Fisher, Carlsbad, CA, USA), 11-*cis*-retinal (National Eye Institute, Bethesda, MD, USA), siRNA (Dharmacon, Lafayette, CO, USA). Reagents were dissolved in appropriate solvents according to manufacturer's instructions. HeLa cells were originally purchased from the American Tissue Culture Collections (ATCC, Manassas, VA, USA) and authenticated using a commercial kit to amplify 9 unique STR loci. SKOV3, MDA-MB231, and HCT116 cell lines and control siRNA were kindly provided by Dr. Deborah N. Chadee, University of Toledo, Toledo, OH. NCI-H125 cell line was kindly provided by Dr. Randall Ruch, University of Toledo, Toledo, OH.

2.2. Cell culture and transfections

HeLa cells (ATCC) were cultured in minimum essential medium (MEM, Gibco) containing 10% dialyzed fetal bovine serum (DFBS, Atlanta Biologicals), in the presence of 1% penicillin-streptomycin (PS, Corning) in tissue culture dishes (60 mm, 100 mm) in a humidified incubator at 37 °C, 5% CO_2. At 80% confluency, HeLa cells were treated with versene-EDTA (CellGro) and incubated for 2 min at 37 °C. Dislodged cells were lifted and centrifuged at 1000*g* for 3 min and versene-EDTA was immediately aspirated before resuspending in MEM with 10% dialyzed fetal bovine serum. One day before the transfection of DNA, 0.8×10^5/ml HeLa cells were seeded on 35 mm glass bottom dishes (In Vitro scientific). Transfections were performed using Lipofectamine 2000 according to manufactures protocol and imaging was performed next day after transfection. Similarly, SKOV3, MDA-MB231, and HCT116 were cultured in Dulbecco's Modified Eagle's Medium (DMEM, Corning) containing 10% DFBS and 1% PS and NCIH125 cell line was cultured in Roswell Park Memorial Institute (RPMI-1640, Gibco) containing 10% DFBS and 1% PS. Rest of the cell culture, seeding and transfection procedures for all the cell lines were similar to the protocols described for HeLa cells.

2.3. siRNA transfection to knock down Gαs in HeLa

To efficiently knock down GNAS in HeLa, siRNA sequence CGAUG UGACUGCCAUCAUC was used as described previously [65]. siRNA was dissolved in RNase-free 1× siRNA buffer and concentration was verified using NanoDrop microvolume spectrophotometer. siRNA (50 nM) was introduced to HeLa cells using Lipofectamine 2000 (Thermo Fisher) transfection reagent. Control siRNA transfected HeLa cells were used as the control.

2.4. RNAseq, real time PCR and cancer cell line encyclopedia (CCLE) data analysis

Access to RNAseq data for HeLa were provided by Professor N. Gautam, Washington University. Relative expression of GNA subunits was calculated after normalized to expression of α-tubulin. Relative expression of GNA subunits was expressed as standard deviation and plotted in Origin pro (OriginLab Corporation). CCLE contains mRNA expression data for > 1000 cancer cell lines. GENE-E, Java desktop application developed by Broad institute (Cambridge, MA, USA) was used to generate GNA gene expression heat maps with respect to GAPDH for SKOV3, and HCT116. To obtain the Gαs and Gαq/11 expression profile of MDA-MB231 and NCI-H125, cells cultured in 100 mm tissue culture dishes with their appropriate media. When cells reached to ~80% confluency, cells were then homogenized to isolate total mRNA using GeneJET RNA purification kit. cDNA synthesis performed with 2.5 μg total RNA using RADIANT cDNA synthesis kit. The GNA expression was quantified by real-time PCR using RADIANT Green LO-ROX qPCR kit. Real time amplification was carried out using Icycler (BIO-RAD, Hercules, CA). Quantification of GNA expression was performed against β-actin internal control as previously described [66].

2.5. Western blot analysis

Whole cell extracts were prepared from NCI-H125, HeLa and MDA-MB-231 cells and separated by 15% SDS polyacrylamide gel electrophoresis. Proteins were then transferred to a PVDF membrane, blocked with 5% non-fat milk, and incubated with the primary antibodies (Santa Cruz Biotechnology) specific for Gαs (sc-135914), Gαq (sc-136181) and α-tubulin (sc-53646), followed by the appropriate HRP-conjugated secondary antibody (Bio-Rad: #1705047). The membrane was incubated with chemiluminescent detection solutions (MilliporeSigma Corporation: WBKLS0500) and exposed to an X-ray film. The protein band intensities on X-ray films were quantified using

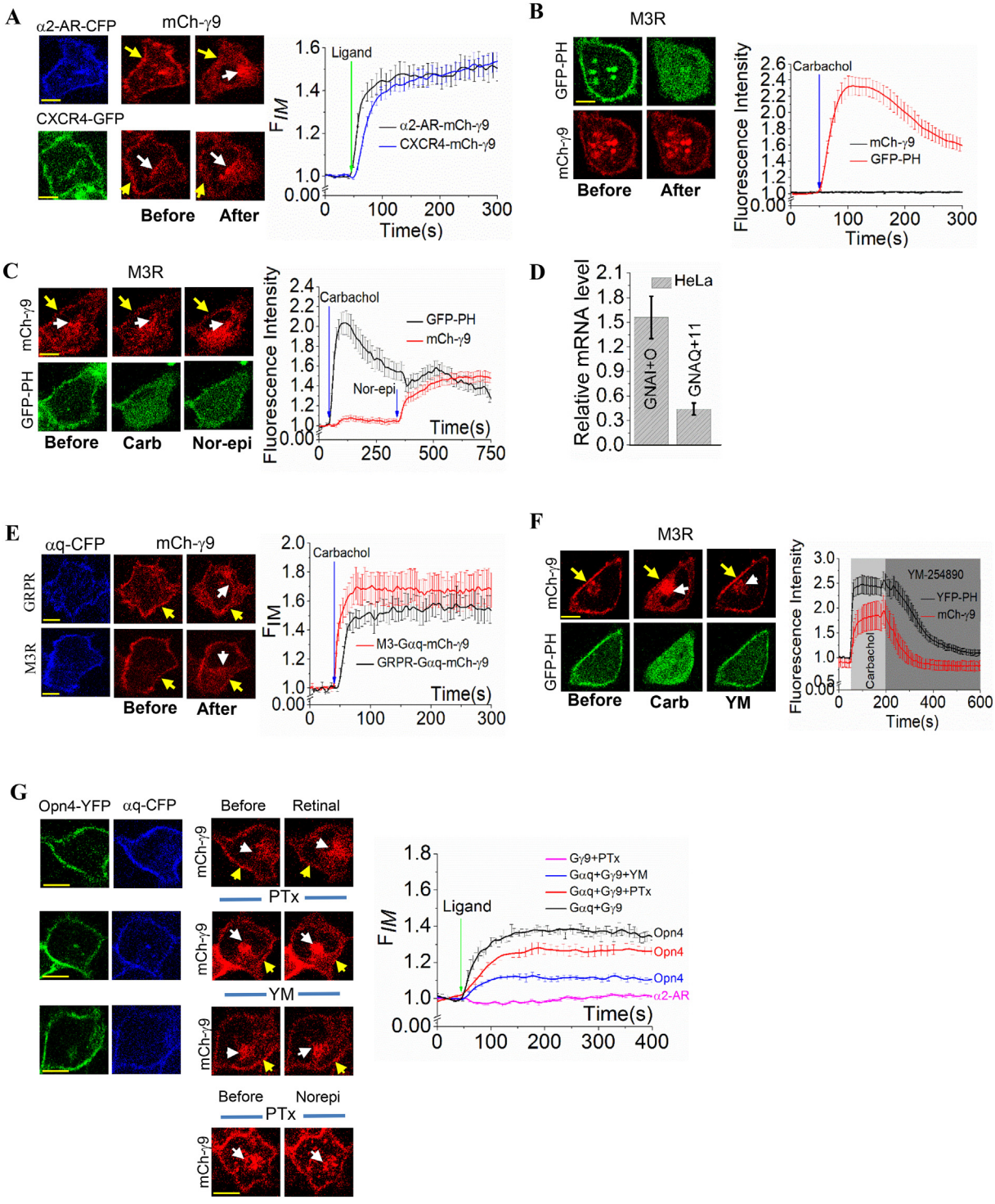

Fig. 1. Compared to robust-Gβγ translocation exhibiting Gi/o-GPCRs, Gq-GPCR activation results in a limited Gβγ generation. (A) HeLa cells exhibited profound mCherry-g9 translocations upon activation of α2-AR-CFP (with 50 μM norepinephrine) as well as CXCR4-GFP (with 50 ng/mL SDF-1α). Corresponding plots show the extent of Gγ9 translocation measured using fluorescence change in IMs (white arrows). (B) HeLa cells expressing M3R, GFP-PH, and mCherry-γ9 failed to show Gγ9 translocation upon M3R activation with 10 μM carbachol although cells did exhibit the characteristic Gq-mediated PIP2 hydrolysis. (C) In a similar experiment to B, after ~5 min of carbachol addition, cells were treated with 50 μM norepinephrine, and cells exhibited Gγ9 translocation. (D) Normalized mRNA expression of GNAI +O and GNAQ+11 in HeLa cells: Values were normalized to α-tubulin (E) HeLa cells expressing Gαq-CFP, mCherry-γ9 with either M3R or GRPR showed characteristic Gγ9 translocation upon addition of their respective ligand. (F) In a similar experiment to E, ~200 s after M3R activation, addition of 1 μM Gq inhibitor, YM-254890 immediately reversed the Gγ9 translocation and PIP2 hydrolysis, restoring their distribution to pre-activation conditions. (G) HeLa cells expressing Opn4-YFP, Gαq-CFP, and mCherry-γ9 showed a profound Gγ9 translocation upon activation by adding 50 μM 11-*cis* retinal while imaging. HeLa cells expressing Opn4-YFP, Gαq-CFP, and mCherry-γ9 additionally treated with 50 ng/mL PTx showed Gγ9 translocation upon Opn4 activation. When cells were treated with 1 μM YM-254890, still Gγ9 translocation was observed, however to a lesser extent. HeLa cells expressing mCherry-γ9 treated with PTx failed to induce Gγ9 translocation, α2-AR activation suggesting that PTx treatment completely inhibits Gi-pathway activation. Corresponding plot shows fluorescence intensity changes in IMs (mCh-γ9) PM (yellow arrows) and IMs (white arrows). Scale bar:10 μm. Average curves plotted using $n \geq 10$ cells from ≥3 independent experiments. Error bars: SEM. (For interpretation of the references to colour in this figure legend, the reader is referred to the web version of this article.)

NIH ImageJ. The values for Gα subunits were normalized to the α-tubulin loading control. Statistical analysis of immunoblots was performed by Students *t*-test on three independent biological replicates. A *p*-value < .05 was considered statistically significant.

2.6. The Cancer Genome Atlas (TCGA) data analysis

The Cancer Genome Atlas (TCGA) cohort data available in the Genomic Data Commons (GDC) data portal was used in this study in May 2018. RNAseq raw counts of 10,455 samples across 33 cancer types were downloaded using the R/Bioconductor package TCGA biolinks version 2.5.9 [67] using GDC prepare for tumor types (level 3, and platform "IlluminaHiSeq_RNASeqV2"), "data.type" as "Gene expression quantification" and "file.type" as "results". The resulting data were the raw gene expression RSEM values generated by TCGA pipeline which uses MapSplice [68,69] to do the alignment and RSEM to do the quantification [69,70].

2.7. Imaging and data analysis

A Nikon-Andor spinning disc confocal imaging system, composed of a Nikon Ti-R/B inverted microscope, a Yokogawa CSU-X1 spinning disk (5000 rpm) and iXon ULTRA 897BV back illuminated deep-cooled EMCCD camera was used. All DNA constructs were transiently transfected, and cells were imaged next day after the transfection. M3R and GRPR untagged expression were confirmed by PIP2 hydrolysis or Gβγ translocation in the presence of αq-CFP. Imaging of cells were carried out using a 60×, 1.4 NA oil objective employing 50 mW 445, 488, 515 and 595 nm solid-state lasers. Sensors were imaged using the following settings: GFP-PH and PKCδ-GFP: 488 nm at 56 μW/515 nm, YFP-PH,Opn4-YFP and GRK2-YFP: 515 nm at 22 μW/540 nm; mCherry-γ9 and mCherry-PH: 594 nm at 20 μW/630 nm, α2-AR-CFP,β1-AR-CFP and αq-CFP: 445 nm at 196 μW/482 nm (excitation/emission). All the ligands mentioned in the manuscript, added to cells at 50 s unless otherwise specified. Imaging of PIP2 sensors, PKCδ and translocation of Gγ1, 9, and 11 were also performed at 1 Hz. GPCR activation induced Gβγ translocation reduce fluorescence of the tagged Gγ on the PM and increase in IMs. Therefore, fluorescence increase in IMs (F_{IM}) was used to measure the extent of heterotrimer dissociation upon GPCR activation. Digital image analysis was performed using Andor iQ 3.1 software and fluorescence intensity obtained from regions of interest (PM, IMs and cytosol) were normalized to initial values (baseline) in MS excel. Normalized data were then plotted using Origin pro (OriginLab Corporation). Results of all quantitative assays (Gβγ translocation, PKCδ and GRK2 recruitment and PIP_2 hydrolysis) are expressed as standard error of mean (SEM) from *n* numbers of cells (indicated in the figure legends) from multiple days, using cells with different passage numbers.

3. Results and discussion

3.1. Endogenous Gαq activation in HeLa cells exhibits a reversible PIP2 hydrolysis and comparatively limited free Gβγ generation

The objective was to examine molecular reasonings behind the inability of Gq-coupled GPCRs (Gq-GPCRs) to induce a detectable Gγ9 translocation in HeLa cells upon activation. We previously established translocation of fluorescently tagged Gγ9 can be used to monitor Gi/o and Gs coupled GPCR-G protein activation [58]. We also showed that all Gβγ complexes translocate upon receptor activation while translocation rates are Gγ-type dependent [3,43]. Since Gγ9 containing Gβγ translocate the fastest, we comparatively examined fluorescently tagged Gγ9 translocation after Gi/o- as well as Gq-GPCR activation. HeLa cells expressing mCherry-γ9 were activated with either 50 μM norepinephrine or 50 ng/mL stromal derived growth factor 1-α (SDF1-α) to activate Gi-coupled alpha 2-adrenergic receptors (α2-ARs) and CXCR4 receptors, respectively. Activation of both Gi-coupled GPCRs induced Gγ9 translocation from the PM (yellow arrow) to internal membranes (IMs, white arrow) (Fig. 1A). Quantification of this translocation is provided in the method section. During time-lapse confocal imaging, ligands were added at 50 s to activate the corresponding GPCRs (Fig. 1A, plot). Similarly, HeLa cells expressing mCherry-γ9 and GFP-PH (PIP2 sensor) together with either Gq-coupled Muscarinic 3 (M3) or Gastrin-releasing peptide (GRP) receptors were activated with their corresponding ligands, 10 μM carbachol and 1 μM bombesin, respectively. Upon activation of either receptors, cells did not show a detectable Gγ9 translocation while exhibited the characteristic PIP2 hydrolysis followed by its recovery (PIP2 regeneration over time) (Fig. 1B and S1). The reported enhanced GTPase activity of Gαq-GTP activated-PLCβ also induces fast hydrolysis of GαqGTP and accelerates deactivation of G protein signaling [71,72]. Since the receptors are active and continue to generate Gαq-GTP, fast GTP hydrolysis on Gαq is unlikely to induce the recovery of PIP2. Nevertheless, this prediction requires further investigation. Interestingly, HeLa cells that failed to show translocation of Gγ9 upon M3R activation exhibited a robust Gγ9 translocation after activating endogenous α2-AR (Fig. 1C). This suggests that Gi/o heterotrimers are abundant and functional in these cells. To eliminate the potential influence of the level of receptor expression on Gβγ translocation, HeLa cells with the similar expression levels of CXCR4- and GRPR- GFP tagged versions were selected and activated with their respective ligands to examine mCherry-γ9 translocation. Under these conditions, only CXCR4 showed Gγ9 translocation while GRPR failed to show the Gγ9 translocation (Fig. S2). To examine Gβγ translocation at equivalent levels of Gαo and Gαq, HeLa cells transfected αo-mCherry and αq-CFP with near similar expressions were used. Upon activation of α2-AR and GRPR with their respective ligands, the observed Gγ9 translocation rates in Gαo ($0.035\ s^{-1}$) and Gαq ($0.027\ s^{-1}$) cells were nearly similar (Fig. S3).

We examined whether observed lack of Gγ9 translocation upon Gq-coupled ligand-binding GPCR activation was due to limited availability of Gq-heterotrimers in HeLa cells. Interestingly, RNAseq profile for Gα shows that HeLa cells express a relatively higher amount of GNAI + O compared to GNAQ + 11 (Fig. 1D). Therefore, Gβγ is likely to form a limited amount of Gq/11 heterotrimers. To increase the relative abundance of Gαq compared to endogenous Gαs and Gαi/o, HeLa cells expressing mCherrry-γ9, M3R or mCherry-Gγ9, GRPR were also co-transfected with αq-CFP. Upon activation of M3R as well as GRPR, cells exhibited robust translocations of mCherry-γ9 (Fig. 1E). These translocation responses ($Tt_{1/2}$ M3R = 6 ± 1 s and $Tt_{1/2}$ GRPR = 7 ± 1 s) were similar to the γ9 translocation observed upon Gi-coupled GPCR activation ($Tt_{1/2}$ α2-AR = 7 ± 2 s) (Fig. 1A). Therefore, this data clearly indicates that the lack of Gγ9 translocation observed in HeLa cells with endogenous Gαq is likely due to the limited availability of Gq-heterotrimers and unlikely due to the inefficient Gq-heterotrimer activation. However, PLCβ mediation of accelerated GTP hydrolysis on Gαq can also play a role here. When cells were treated with 1 μM YM-254890 at 200 s, a complete reverse of Gγ9 translocation back to the PM and complete reverse translocation of the PIP2 sensor to the PM were observed after M3R activation in HeLa cells expressing αq-CFP (Fig. 1F). This data clearly demonstrate that observed Gγ9 translocation in Gαq expressing cells is solely governed by Gq-heterotrimer activation. Whether or not the lack of translocation observed upon Gq-pathway activation is unique to Gγ9 was also examined. HeLa cells transiently expressing M3R and either YFP-γ1 or YFP-γ11 did not show γ1 and γ11 translocation upon addition of 10 μM carbachol (Fig. S4A). However, HeLa cells additionally expressing αq-CFP exhibited significant γ1 and γ11 translocations from PM (yellow arrow) to IMs (white arrow) upon addition of 10 μM carbachol (Fig. S4B). Introduction of αq-CFP to HeLa cells also induced β1-YFP translocation when cells treated with 10 μM carbachol, which indicates endogenous Gγ translocation (Fig. S4B). Therefore, the reason not all Gγ types translocate in HeLa cells upon Gq-coupled GPCR activation is the limited

availability of Gq-heterotrimers.

We recently showed that melanopsin (Opn4) is promiscuous to both Gi/o- and Gq-pathway with near similar efficiencies [63]. HeLa cells expressing Opn4, mCherry-γ9 and YFP-PH exhibited both Gγ9 translocation and PIP2 hydrolysis in the presence of 50 μM 11-*cis* retinal (Fig. S5A). In the presence of 50 ng/mL pertussis toxin (PTx), Opn4 activation only exhibited PIP2 hydrolysis and failed to show Gγ9 translocation (Fig.S5B). When Opn4 expressing cells were treated with Gq inhibitor (YM-254890), which blocks Gq-heterotrimer dissociation by preventing GDP/GTP exchange [73], Opn4 activation induced Gγ9 translocation while no PIP2 hydrolysis was observed (Fig.S5C). Therefore, we utilized Opn4 to show that levels of Gq- and Gi/o-heterotrimer activation by the same receptor with nearly similar promiscuity is controlled by the concentrations of Gα subtypes. HeLa cells expressing Opn4, αq-CFP and mCherry-γ9 exhibited a profound Gγ9 translocation upon Opn4 activation (by adding 50 μM 11-*cis* retinal) (Fig. 1G-top, black curve). The observed translocation in Gαq expressing cells is due to both Gαi- and Gαq-heterotrimer activation. When HeLa cells treated with 50 ng/mL PTx for 6 h, Opn4 activation still induced Gγ9 translocation, however to a lesser extent (Fig. 1G-middle, red curve). Gq-inhibitor, YM-254890, treated cells also exhibited Gγ9 translocation upon Opn4 activation, however to a much lesser extent compared to cells untreated as well as cells treated with 50 ng/mL PTx (Fig. 1G bottom, blue curve). Since Gαq introduction to HeLa cells is likely to increase Gαq compared to Gαi/o, this greater reduction of Gγ9 translocation by YM-254890, compared to that of PTx, is expected. Additionally, complete lack of Gγ9 translocation in PTx treated HeLa cells upon activation of endogenous α2-AR show that, Gγ9 translocation observed in PTx-treated cells is primarily due to Gq-pathway activation. (Fig. 1G, magenta curve). Nearly similar Gβγ translocation rates in untreated ($0.010\,s^{-1}$), PTx treated ($0.005\,s^{-1}$) and YM treated ($0.006\,s^{-1}$) cells suggest that both Gq and Gi/o heterotrimer processing rates are nearly similar, and the extent is dictated by the respective heterotrimer concentrations. These results also help to speculate that the lack of Gβγ translocation induced by M3R activation in HeLa cells (Fig. 1B) is likely due to limited Gq-heterotrimer activation as a result of the relatively lower abundance of Gαq compared to other Gα types. Nevertheless, there are some variabilities in heterotrimer activation even by the same GPCR when activated with different ligands. We have demonstrated this using distinct Gβγ translocation abilities of norepinephrine and tizanidine in HeLa cells upon endogenous α2-AR activation [58]. Therefore, the differences observed in translocation extents as well as rates can be partially due to varying efficiencies of heterotrimer activation by distinct receptors as well as ligands. We anticipate such differences among receptor families that activate different heterotrimers such as Gs and Gq to be more prominent. However, we do not anticipate such differences to induce or eliminate sufficient free Gβγ generation and their translocation.

3.2. Gαq transfected cells exhibit distinct signaling compared to cells with endogenous Gαq

3.2.1. PIP recovery

Although HeLa cells only expressing endogenous Gq subunits was unable to exhibit Gβγ9 translocation, they showed an efficient PIP2 hydrolysis upon Gq-pathway activation (Fig. 1B, Fig. S1). Interestingly, within minutes of this PIP2 hydrolysis, the PIP2 sensor returned to the PM, indicating PIP2 regeneration at the PM. Therefore, we examined if Gq-pathway induced PIP2 hydrolysis-responses in HeLa cells with and without Gαq transfection are comparable. HeLa cells expressing M3R, αq-CFP, and GFP-PH exhibited a robust PIP2 hydrolysis upon addition of 10 μM carbachol (Fig. 2A-top, red curve). However, no recovery of PIP2 was observed, even after 15 min of M3R activation. Interestingly, under similar conditions, control cells (no Gαq transfection) exhibited PIP2 recovery after 5–6 min of M3R activation (Fig. 2A-bottom, black curve). A similar experiment was performed in HeLa cells expressing GRPR, αq-CFP, and mCherry-PH to eliminate receptor specific recovery of PIP2 hydrolysis. Upon activation of GRPR with 1 μM bombesin, cells failed to exhibit PIP2 recovery even after 15 min (Fig. 2B- top, red curve), while control cells exhibited the recovery of PIP2 (Fig. 2B-bottom, black curve). These data thus confirm that elevated levels of Gαq expression alters the signaling outcome of Gq-pathway activation.

3.2.2. PKC recruitment

Gq-pathway activation and subsequent DAG formation at the PM induces PM recruitment and activation of cytosolic PKC isoforms [74,75]. When the recovery of PIP2 hydrolysis incurs, as it consumes DAG to resynthesize PIP2, PKC is expected to return to the cytosol. We examined whether this PKC recruitment-activation process is altered in cells transfected with Gαq. HeLa cells transiently expressing M3R, αq-CFP, and PKCδ-GFP exhibited no reversal of PM recruited PKCδ to the cytosol even after 20 min (Fig. 2C-top, red curve). Cells lacking Gαq-transfection exhibited both PM recruitment and reversal of PKCδ (Fig. 2C-bottom, black curve). Similar ro M3R, HeLa cells expressing GRPR also exhibited a similar dependency of PKCδ-GFP translocation-reversal upon activation (Fig. 2D). These data suggest that excessive Gαq-heterotrimer activation disrupts PIP2 recovery process that is likely to control the signaling outcome of the Gq-pathway.

3.2.3. GRK2-GPCR interaction

Signaling of activated GPCRs are attenuated by receptor desensitization and internalization [76–78]. G protein regulated kinase 2 (GRK2) has been shown to translocate to the PM from the cytosol to phosphorylate several GPCRs including M3R to initiate their desensitization and internalization [79]. We examined whether a detectable PM-recruitment of GRK2 can be observed with endogenous Gαq. HeLa cells expressing M3R and GRK2-YFP did not exhibit a profound recruitment of GRK2 when M3R was activated (Fig. 2E-bottom, black curve). Nevertheless, HeLa cells additionally expressing αq-CFP exhibited a robust GRK2 recruitment to PM after M3R activation (Fig. 2E-top, red curve). This suggests that the excessive Gq-heterotrimer activation and Gq signaling is likely to induce enhanced phosphorylation of GPCRs, accelerating their desensitization. GRK2 recruitment to activated GPCRs require Gβγ and Gαq [79,80]. Since Gi/o coupled α2-AR activation induces GRK2 recruitment to the PM [81], we examined the role of Gβγ in PM recruitment of GRK2 in HeLa cells treated with and without Gβγ-inhibitor, gallein. Upon addition of norepinephrine (50 μM) cells exhibited profound translocation of GRK2 to the PM (Fig. 2F-top, black curve). HeLa cells exposed to 10 μM gallein for 15 min showed a significantly reduced PM recruitment of GRK2 (Fig. 2F-bottom, red curve). These data suggest that free Gβγ generation upon α2-AR activation is required for GRK2 recruitment. To examine if Gβγ similarly involved in Gq-pathway activation-induced GRK2 recruitment, HeLa cells expressing M3R, αq-CFP, and GRK2-YFP were examined with and without 10 μM gallein exposure. Compared to gallein untreated cells, GRK2 recruitment in gallein treated cells was marginal (Fig. 2G). These data collectively indicate that Gαq-expression level-dependent generation of Gβγ involves in signaling regulation of Gq-pathway.

3.3. Gβγ translocation reflects the level of Gαq expression

Since Gq-pathway activation in HeLa cells show Gβγ translocation only with Gαq overexpression while Gs-pathway activation shows Gβγ translocation with endogenous Gαs, we examined the level of Gαs and Gαq protein in HeLa cells (Fig. 3A). Protein expression data normalized to α-tubulin from HeLa cells show that, compared to Gαs, the Gαq expression is significantly lower (Fig. 3A, bar chart). Thus, translocation data indicate that the limited availability of endogenous Gαq to form heterotrimers in HeLa cells is likely to result in a Gγ9 translocation which cannot be detected by confocal microscopy (Fig. 1B). Gαq transfection to HeLa cells overcomes this limitation, resulting in a

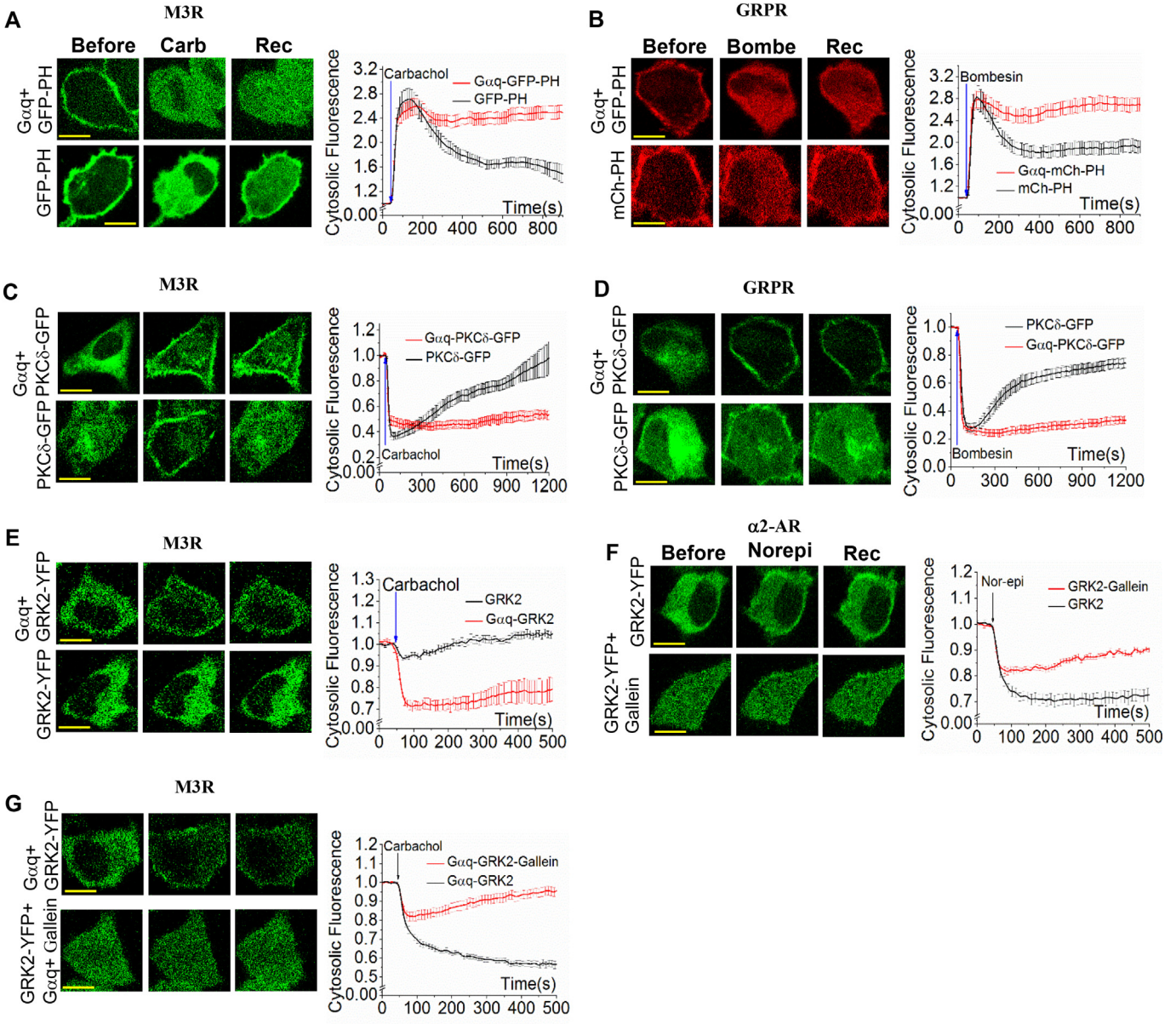

Fig. 2. Gαq transfected HeLa cells exhibited distinct signaling compared to cells with endogenous Gαq. Gαq expressing cells showed irreversible PIP2 hydrolysis after (A) M3R as well as (B) GRPR activation while cells with endogenous Gαq showed a PIP2 hydrolysis which was followed by complete recovery of PIP2 within minutes. (C, D) Gαq transfected cells exhibited an irreversible PKC-recruitment (PKCδ-GFP) to the PM while cells with endogenous Gαq-cells showed a complete return of PKCδ to the cytosol. (E) Gαq transfected HeLa cells exhibited M3R activation induced GRK2 recruitment to the PM while GRK2-YFP remained in the cytosol in control cells lacking Gαq transfection. (F) HeLa cells expressing α2-AR-CFP and GRK2-YFP showed robust GRK2 recruitment to PM upon addition of 50 μM norepinephrine while cells incubated with 10 μM gallein showed a significant reduction in GRK2 recruitment to the PM. (G) HeLa cells expressing M3R, αq- CFP, and GRK2-YFP additionally treated with 10 μM gallein, exhibited reduced GRK2 recruitment upon M3R activation compared to control HeLa cells (no gallein). Note: Scale bar 10 μm. Average curves plotted using n ≥ 10 cells from ≥3 independent experiments. Error bars: SEM.

detectable Gβγ translocation (Fig. 1F). Therefore, we compared the Gβγ translocation after knocking-down an endogenous Gα subunit. Since Gαi/o has multiple isoforms and Gs-GPCR activation induces Gγ9 translocation with endogenous Gαs, we knocked down the Gαs in HeLa using 50 nM siRNA. Compared to control siRNA-cells (Fig. 3B-top, red curve), Gαs knocked-down HeLa cells exhibited only minor Gγ9 translocation (Fig. 3B-bottom, black curve up to 600 s). However, the Gαs knocked-down cells showed profound Gβγ translocation upon activation of endogenous α2-AR, suggesting that knockdown effect of Gαs-siRNA is selective (Fig. 3B-bottom right, black curve from 600 s). These data collectively demonstrate that Gβγ translocation is an indicator of the level of Gα expression.

3.4. Some cell types endogenously express higher levels of Gαq and possess distinct Gq-pathway signaling

Real time PCR data of NCI-H125 lung carcinoma cells showed a ~50% higher expression of GNAQ/11 compared to MDA-MB 231 (Fig. 4A). Therefore, we comparatively examined how relative expression Gαq is connected to Gβγ translocation and, Gq-pathway signaling in MDA-MD 231 (breast cancer) cells, and NCI-H125 (human Adenosquamous lung carcinoma) cells. We first examined their relative Gαq levels in both cell lines. Western blot data showed that Gαq expression in NCI-H125 cells was significantly higher than that of MDA-MB 231 cells (Fig. 4B, bar chart). Next, we examined Gq-pathway activation induced Gβγ translocation in both the cell types. As

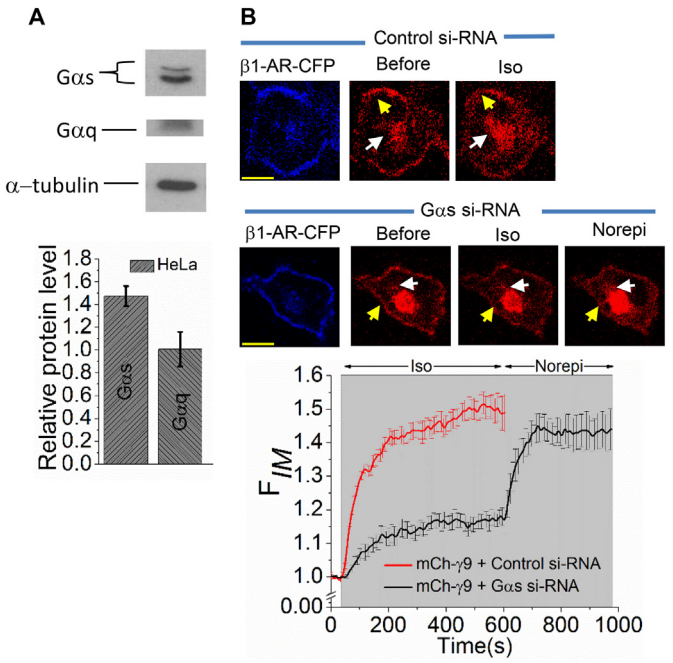

Fig. 3. Knockdown of Gαs reduces Gs-pathway induced Gβγ translocation. (A) Western blot quantification showed the level of Gαs expression in HeLa cells is significantly higher than Gαq. Gαs and Gαq expression level data normalized to α-tubulin. (Error bars = SD, $n = 3$ independent experiments, $p < .05$). (B) HeLa cells transfected with β1-AR-CFP, mCherry-γ9 and control siRNA, exhibited a profound Gγ9 translocation upon addition of 20 μM isoproterenol. HeLa cells transfected with siRNA for Gαs only exhibited ~30% of the Gγ9 translocation compared to control siRNA cells. Suggesting the specificity of Gαs siRNA, cells were then treated with 50 μM norepinephrine (at 600 s) to activate endogenous α2-AR, cells exhibited a robust Gγ9 translocation. Corresponding plots show the fluorescence intensity change in IMs (mCh-γ9). Note: PM (yellow arrows) and IMs (white arrows). Scale bar:10 μm. Average curves plotted using n ≥ 10 cells from ≥3 independent experiments. Error bars: SEM. (For interpretation of the references to colour in this figure legend, the reader is referred to the web version of this article.)

anticipated, M3R activation in MDA-MB-231 cells exhibited the characteristic PIP2 hydrolysis and subsequent recovery (Fig. 4C-top, black curve). These cells also failed to show a detectable Gγ9 translocation (Fig.-4D top, red curve). Upon M3R activation in cells additionally expressing Gαq, cells exhibited a robust Gγ9 translocation (Fig. 4D-bottom, black curve) as well as recovery resistant PIP2 hydrolysis (Fig. 4C bottom, red curve). Interestingly, activation of M3R in NCI-H125 cells resulted in both irreversible PIP2 hydrolysis (Fig. 4E-top, black curve) and mCherry-γ9 translocation (Fig. 4F-top, red curve). When NCI-H125 cells were additionally transfected with αq-CFP, cells exhibited ~two times higher extent of Gγ9 translocation than the response observed in cell with endogenous Gαq (Fig. 4F-bottom, black curve). Nevertheless, PIP2 hydrolysis responses observed in Gαq transfected cells and cells with endogenous Gαq were nearly similar and irreversible (Fig. 4E, plot). Similarly, we selected SKOV3 (adenocarcinoma) and HCT116 (colorectal carcinoma) cell lines by examining their relative Gαq/11 expression levels from CCLE. Both SKOV3 and HCT116 expressed low amount of GNAQ and GNA11 compared to GAPDH, housekeeping gene (Fig.S6A) Therefore, we anticipated that these cell types express relatively low amounts of Gαq, and possess low abundance of Gq-heterotrimers to interact with Gq-GPCRs. To validate these observations, we examined Gγ9 translocation and PIP2 hydrolysis in these two cell types transfected with M3R, mCherry-γ9, and YFP-PH. Upon activation of M3R, both the cell lines exhibited the characteristic PIP2 hydrolysis and subsequent recovery (Fig. S6B and C, I, top). However, they did not show a detectable Gγ9 translocation (Fig. S6B and C, II, top). Interestingly, upon additionally expressing Gαq-CFP, both cell lines exhibited Gγ9 translocation on M3R activation (Fig. S6B and C, II, bottom). Further, PIP2 hydrolysis in Gαq transfected cells were irreversible, indicating lack of recovery (Fig. S6B–C, I, bottom). These data clearly show that elevated expression of Gαq/11 is physiologically relevant and characterized by distinct signaling regimes. We also observed from transcriptome data that, in addition to lung carcinoma, several breast, ovarian, and pancreatic cancer cells lines possess elevated levels of Gαq/11 mRNA, indicating a broader physiological relevance.

3.5. Elevated expression of GNAQ/11 is found in human cancer

Since endogenously elevated Gαq expression as well and Gαq overexpression result in a distinct signaling regime for Gq-pathway activation in cells, we examined GNAQ expression levels in specific tumors compared to its expression levels in normal tissues of the same patient. This investigation was further encouraged by the identification of GNAQ and 11 as cancer driver genes [60,61]. The Cancer Genome Atlas (TCGA) data includes over 10,000 tumors from 33 cancer types and helps to expand the current understanding of oncogenesis [82]. Specially tumor-normal exome pairs allow us to compare the expression of GNAQ (Gαq) in human cancers compared to normal samples from the same patient. To find the contrast between gene expression in normal (blood or adjacent normal) to primary tumor tissue, we filtered data to find 669 patients (20 cancer types) where both normal and primary tumor expression data were available. Then, for each cancer type, GNAQ expression values for matched normal and primary tumor samples were used to perform a Wilcoxon signed-rank test for paired observables. For each cancer type, a *p*-value is generated by the aforementioned test with null hypothesis being the distribution of GNAQ expression in tumors subtracted from normal samples is symmetric about the mean, while the alternative hypothesis being GNAQ expression of tumors is higher than the normal samples (Fig. 5). Moreover, to compare and visualize tumor vs normal GNAQ expression case by case, we calculated the ratio of tumor over normal expression for each patient. We found that while many cancer types like bladder urothelial carcinoma (BLCA), breast invasive carcinoma (BRCA), head and neck squamous cell carcinoma (HNSC), and liver hepatocellular carcinoma (LIHC) exhibited a considerable fraction of patients having higher GNAQ expressions in tumors compared to the matched normal. Kidney chromophobe (KICH) and kidney renal papillary cell carcinoma (KIRP) patients showed that a significant fraction of patients has a higher GNAQ expression in tumor compared to matched normal (*p* values 0.00007 and 0.0041 respectively). We also examined the matched tumor and normal expressions and their ratios for BRCA (as a control), KICH and KIRP cancer types (Fig. 5A). Matched tumor-normal expression data were available for 112, 25, and 32 patients in BRCA, KICH, and KIRP respectively (Fig. 5B). Therefore, the cancer cohort data suggest that KICH and KIRP cancer patients can be susceptible for elevated levels of Gαq mediated signaling.

4. Conclusions

Regulation of the active states of Gαq-GTP and PLCβ as well as their control of dependent pathways provide pivotal regulation of many molecular processes in cells that are crucial for cellular homeostasis and survival. Hence, the Gq-pathway is majorly implicated in debilitating and deadly diseases including diabetes, heart diseases, and cancer. Therefore, delineating processes that regulate Gαq-GTP and PLCβ signaling is not only fundamental to understand mammalian physiology, but also to develop therapeutics. In summary, our data suggest that many cell types express relatively low Gαq levels compared to other Gα types such as Gαs and generate a limited amount of Gβγ, indicated by the lack of a detectable Gβγ9 translocation upon Gq-pathway activation. In these cells, the resultant PIP2 hydrolysis was transient and cells

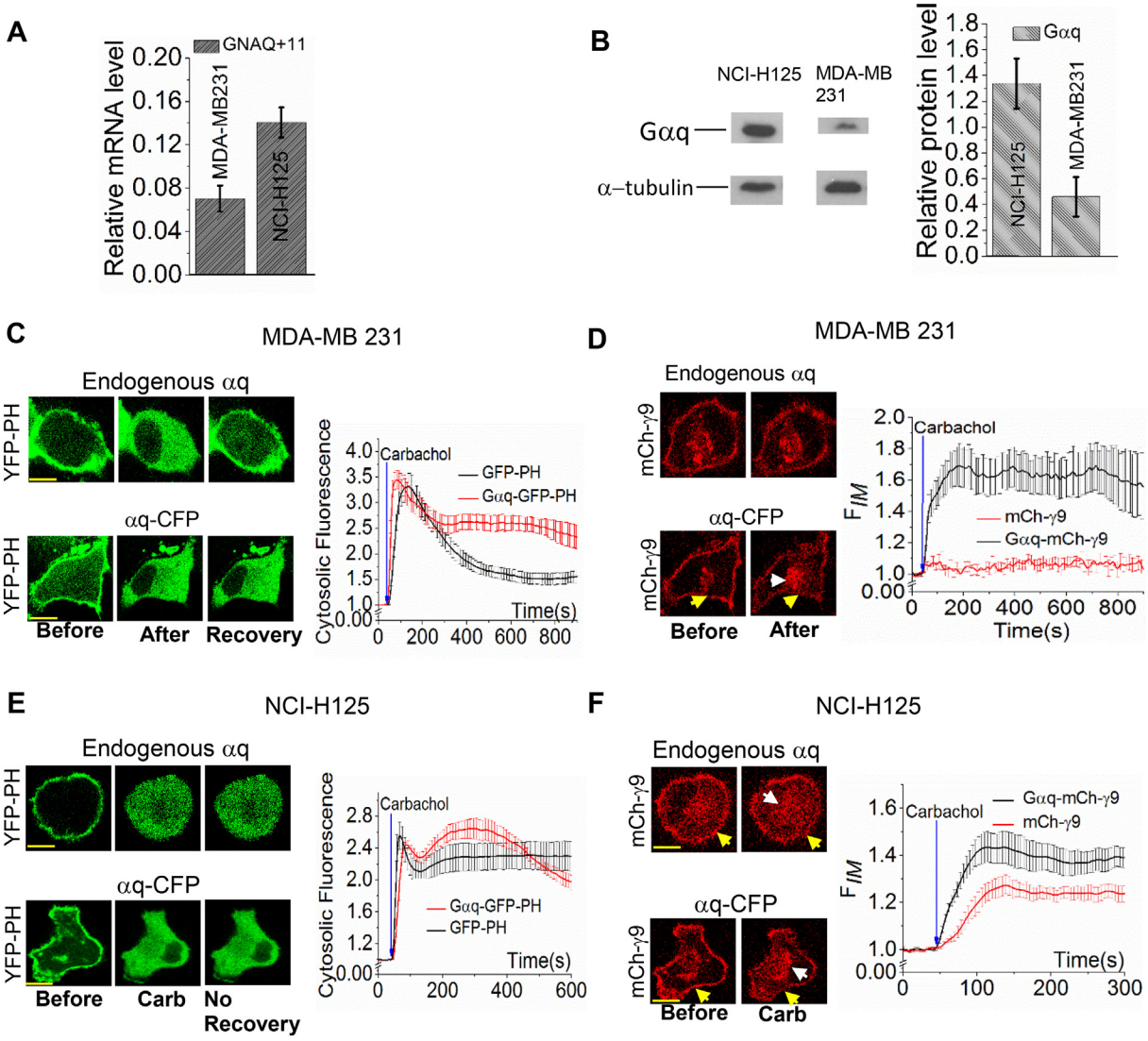

Fig. 4. NCI-H125 lung carcinoma cells endogenously expresses higher Gαq levels compared to MDA-MB-231 breast cancer cells and also exhibited distinct Gq-signaling. (A) Real time PCR data showed higher Gαq/11 in NCI-H125 compared to MDA-MB231. (Error bars = SD, n = 3 independent experiments). (B) Western blot analysis showed a higher expression of Gαq in NCI-H125 compared to MDA-MB 231. Protein expression levels normalized to α-tubulin. (Error bars = SD, n = 3 independent experiments, $P < .05$). MDA-MB231 transfected with M3R (untagged), mCherry-γ9, and YFP-PH – with and without aq-CFP, were subsequently examined for M3R activation induced, (C) PIP2 hydrolysis and (D) Gγ9 translocation. Corresponding plots exhibit the dynamics of PIP2 hydrolysis and Gγ9 translocation. (E) PIP2 hydrolysis and (F) Gγ9 translocation were examined in NCI-H125 cells under conditions with and without aq-CFP transfection upon M3 activation. Corresponding plots exhibit PIP2 hydrolysis and Gγ9 translocation dynamics. Note: Gγ9 translocation from the PM (yellow arrows) to IMs (white arrows). Average curves plotted using n ≥ 10 cells from ≥3 independent experiments. Error bars: SEM. Scale bar:10 μm. (For interpretation of the references to colour in this figure legend, the reader is referred to the web version of this article.)

were unable to recruit detectable levels of GRK2 to activated GPCRs on the PM. Contrarily, both Gαq transfected cells as well as cells endogenously expressing relatively higher Gαq levels exhibited robust Gβγ translocations and recovery-resistant PIP2 hydrolysis. The discovery of the GTPase activity of PLCβ for GαqGTP unveiled the faster physiological deactivation of G protein signaling [72,83]. With the identification of GNAQ (Gαq) as a cancer driver gene and our data demonstrating Gαq-expression dependent signaling regimes indicate that the regulation of Gq-expression is another mechanism that cells employ to achieve desired signaling outcomes. Our findings may also provide molecular explanations for Gq-pathway involvement in certain cancers.

Data availability statement

The CCLE data is available at an integrated portal on www.broadinstitute.org/ccle repository and TCGA data is available in NIH cancer institute GDC data portal.

Conflicts of interest

The authors declare that there is no conflict of interest regarding the publication of this paper.

Funding statement

This work is supported by the University of Toledo and National Institutes of Health (Grant 1R15GM126455-01A1).

Author contributions

Dinesh Kankanamge conducted majority of experiments and

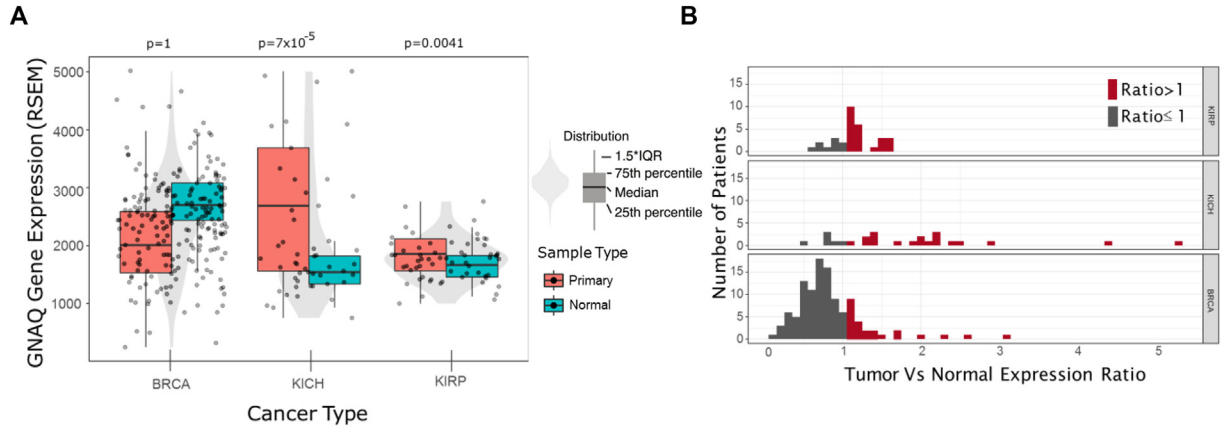

Fig. 5. (A) Elevated GNAQ gene expression in tumor samples compared to normal samples from patients with BRCA (control), KICH and KIRP cancer types. Matched tumor-normal expression data for 112 BRCA, 25 KICH and 32 KIRP patients were extracted from TCGA. Violin plots in the background depict the overall distributions of the GNAQ expression of all the matched tumor and normal samples. Each dot represents the expression value of either a tumor or normal sample. Box plots show the separation of tumor samples from normal samples. In general, GNAQ expression is slightly higher in normal samples of BRCA (used as control) patients, however, patients in KICH and KIRP cohorts show higher GNAQ expression in tumor than in normal samples. This might be an indication of the importance of GNAQ abundance in kidney cancers. (B) Ratio of GNAQ expression in tumor over the matched normal samples in BRCA, KICH, and KIRP. Out of 112, 25, and 32 total number of patients, 27(24%), 19(76%), and 24(75%) patients showed higher GNAQ expression in tumor samples than the matched normal in BRCA, KICH, and KIRP respectively.

analyzed data. Mithila Tennakoon performed RT-PCR and analyzed the data. Amila Weerasinghe analyzed TCGA data. Luis Cedeno-Rosario and Deborah N. Chadee performed the western blot analysis for Gα subunits. Dinesh Kankanamge and Ajith Karunarathne conceived the idea and wrote the manuscript.

Acknowledgements

We acknowledge Prof. N. Gautam for cDNA for G proteins, GPCRs and sensors. We also acknowledge Dr. Deborah N. Chadee, Dr. Randall Ruch for providing cancer cell lines and Dr. Malathi Krishnamurthy for providing the access to RT-PCR. We thank National Eye Institute to provide 11-*cis*-retinal. We also thank Dr. John L. Payton, Dr. Saroopa Samaradivakara, Elise Harmon, Kasun Ratnayake, Kanishka Senarath, and Zehra Fasih for experimental assistance, discussions and comments. We acknowledge University of Toledo for funding.

Appendix A. Supplementary data

Supplementary data to this article can be found online at https://doi.org/10.1016/j.cellsig.2019.02.006.

References

[1] M. Camps, et al., Stimulation of phospholipase C by guanine-nucleotide-binding protein betagamma subunits, Eur. J. Biochem. 206 (3) (1992) 821–831.
[2] S.R. Ikeda, Voltage-dependent modulation of N-type calcium channels by G-protein beta gamma subunits, Nature 380 (6571) (1996) 255–258.
[3] K. Senarath, et al., Ggamma identity dictates efficacy of Gbetagamma signaling and macrophage migration, J. Biol. Chem. 293 (8) (2018) 2974–2989.
[4] T. Clister, S. Mehta, J. Zhang, Single-cell analysis of G-protein signal transduction, J. Biol. Chem. 290 (11) (2015) 6681–6688.
[5] N. Mizuno, H. Itoh, Functions and regulatory mechanisms of Gq-signaling pathways, Neurosignals 17 (1) (2009) 42–54.
[6] L. Zhang, G. Shi, Gq-coupled receptors in autoimmunity, J Immunol Res 2016 (2016) 3969023.
[7] N. Watanabe, et al., Requirement of Galphaq/Galpha11 signaling in the preservation of mouse intestinal epithelial homeostasis, Cell Mol. Gastroenterol. Hepatol. 2 (6) (2016) 767–782 (e6).
[8] N. Wettschureck, A. Moers, S. Offermanns, Mouse models to study G-protein-mediated signaling, Pharmacol. Ther. 101 (1) (2004) 75–89.
[9] S. Mishra, et al., Cardiac hypertrophy and heart failure development through Gq and CaM kinase II signaling, J. Cardiovasc. Pharmacol. 56 (6) (2010) 598–603.
[10] L. Sun, R.D. Ye, Role of G protein-coupled receptors in inflammation, Acta pharmacol. Sin. 33 (3) (2012) 342–350, https://doi.org/10.1038/aps.2011.200.
[11] R.P. Huijbregts, L. Topalof, V.A. Bankaitis, Lipid metabolism and regulation of membrane trafficking, Traffic 1 (3) (2000) 195–202.
[12] M. Manifava, et al., Differential binding of traffic-related proteins to phosphatidic acid- or phosphatidylinositol (4,5)- bisphosphate-coupled affinity reagents, J. Biol. Chem. 276 (12) (2001) 8987–8994.
[13] S. McLaughlin, et al., Adsorption of divalent cations to bilayer membranes containing phosphatidylserine, J. Gen. Physiol. 77 (4) (1981) 445–473.
[14] J.J. Falke, B.P. Ziemba, Interplay between phosphoinositide lipids and calcium signals at the leading edge of chemotaxing ameboid cells, Chem. Phys. Lipids 182 (2014) 73–79.
[15] R.V. Stahelin, J.L. Scott, C.T. Frick, Cellular and molecular interactions of phosphoinositides and peripheral proteins, Chem. Phys. Lipids 182 (2014) 3–18.
[16] T. Nebl, S.W. Oh, E.J. Luna, Membrane cytoskeleton: PIP2 pulls the strings, Curr. Biol. 10 (9) (2000) R351–R354.
[17] D. Holowka, B. Baird, Roles for lipid heterogeneity in immunoreceptor signaling, Biochim. Biophys. Acta 1861 (8 Pt B) (2016) 830–836.
[18] M.P. Czech, PIP2 and PIP3: complex roles at the cell surface, Cell 100 (6) (2000) 603–606.
[19] D.W. Hilgemann, S. Feng, C. Nasuhoglu, The complex and intriguing lives of PIP2 with ion channels and transporters, Sci. STKE 2001 (111) (2001) re19.
[20] M.I. Niemeyer, et al., Phosphatidylinositol (4,5)-bisphosphate dynamically regulates the K2P background K(+) channel TASK-2, Sci. Rep. 7 (2017) 45407.
[21] G.B. Willars, S.R. Nahorski, R.A. Challiss, Differential regulation of muscarinic acetylcholine receptor-sensitive polyphosphoinositide pools and consequences for signaling in human neuroblastoma cells, J. Biol. Chem. 273 (9) (1998) 5037–5046.
[22] C.L. Chang, J. Liou, Phosphatidylinositol 4,5-bisphosphate homeostasis regulated by Nir2 and Nir3 proteins at endoplasmic reticulum-plasma membrane junctions, J. Biol. Chem. 290 (23) (2015) 14289–14301.
[23] M.J. Berridge, Inositol trisphosphate and calcium signalling, Nature 361 (6410) (1993) 315–325.
[24] N. Porciello, et al., Phosphatidylinositol 4-phosphate 5-kinases in the regulation of T cell activation, Front. Immunol. 7 (2016) 186.
[25] S.K. Fisher, Homologous and heterologous regulation of receptor-stimulated phosphoinositide hydrolysis, Eur. J. Pharmacol. 288 (3) (1995) 231–250.
[26] R.J.H. Wojcikiewicz, A.B. Tobin, S.R. Nahorski, Muscarinic receptor-mediated inositol 1,4,5-trisphosphate formation in SH-SY5Y neuroblastoma cells is regulated acutely by cytosolic Ca2+ and by rapid desensitization, J. Neurochem. 63 (1) (1994) 177–185.
[27] M.C. Kienitz, et al., Receptor species-dependent desensitization controls KCNQ1/KCNE1 K+ channels as downstream effectors of Gq protein-coupled receptors, J. Biol. Chem. 291 (51) (2016) 26410–26426.
[28] M.J. Berridge, P. Lipp, M.D. Bootman, The versatility and universality of calcium signalling, Nat. Rev. Mol. Cell Biol. 1 (1) (2000) 11–21.
[29] E. Kania, et al., IP3 receptor-mediated calcium signaling and its role in autophagy in cancer, Front. Oncol. 7 (2017) 140.
[30] V. Veldurthy, et al., Vitamin D, calcium homeostasis and aging, Bone Res. 4 (2016) 16041.
[31] D. Rapaka, et al., Calcium regulation and Alzheimer's disease, Asian Pac. J. Trop. Dis. 4 (2014) S513–S518.
[32] K.T. Kishida, E. Klann, Sources and targets of reactive oxygen species in synaptic plasticity and memory, Antioxid. Redox Signal. 9 (2) (2007) 233–244.
[33] M. Valko, et al., Free radicals and antioxidants in normal physiological functions and human disease, Int. J. Biochem. Cell Biol. 39 (1) (2007) 44–84.
[34] A. Gorlach, et al., Calcium and ROS: a mutual interplay, Redox Biol. 6 (2015) 260–271.

[35] G. Charnogursky, H. Lee, N. Lopez, Chapter 51 - Diabetic neuropathy, in: J. Biller, J.M. Ferro (Eds.), Handbook of Clinical Neurology, Elsevier, 2014, pp. 773–785.
[36] A.B. Hains, et al., Inhibition of protein kinase C signaling protects prefrontal cortex dendritic spines and cognition from the effects of chronic stress, Proc. Natl. Acad. Sci. U. S. A. 106 (42) (2009) 17957–17962.
[37] P. Abrams, et al., Muscarinic receptors: their distribution and function in body systems, and the implications for treating overactive bladder, Br. J. Pharmacol. 148 (5) (2006) 565–578.
[38] S.G. Birnbaum, et al., Protein kinase C overactivity impairs prefrontal cortical regulation of working memory, Science 306 (5697) (2004) 882–884.
[39] Y. Liu, et al., PKCbeta inhibition with ruboxistaurin reduces oxidative stress and attenuates left ventricular hypertrophy and dysfunction in rats with streptozotocin-induced diabetes, Clin. Sci. (Lond.) 122 (4) (2012) 161–173.
[40] K.J. Way, et al., Expression of connective tissue growth factor is increased in injured myocardium associated with protein kinase C 2 activation and diabetes, Diabetes 51 (9) (2002) 2709–2718.
[41] G.J. Digby, et al., Some G protein heterotrimers physically dissociate in living cells, Proc. Natl. Acad. Sci. U. S. A. 103 (47) (2006) 17789–17794.
[42] N.A. Lambert, Dissociation of heterotrimeric g proteins in cells, Sci. Signal. 1 (25) (2008) re5.
[43] W.K. Ajith Karunarathne, et al., All G protein betagamma complexes are capable of translocation on receptor activation, Biochem. Biophys. Res. Commun. 421 (3) (2012) 605–611.
[44] A. Levitzki, S. Klein, G-protein subunit dissociation is not an integral part of G-protein action, Chembiochem 3 (9) (2002) 815–818.
[45] R.V. Rebois, D.R. Warner, N.S. Basi, Does subunit dissociation necessarily accompany the activation of all heterotrimeric G proteins? Cell. Signal. 9 (2) (1997) 141–151.
[46] M. Bunemann, M. Frank, M.J. Lohse, Gi protein activation in intact cells involves subunit rearrangement rather than dissociation, Proc. Natl. Acad. Sci. U. S. A. 100 (26) (2003) 16077–16082.
[47] C. Gales, et al., Real-time monitoring of receptor and G-protein interactions in living cells, Nat. Methods 2 (3) (2005) 177–184.
[48] Kolsch, V., P.G. Charest, and R.A. Firtel, The regulation of cell motility and chemotaxis by phospholipid signaling. J. Cell Sci., 2008. 121(Pt 5): p. 551–9.
[49] W.J. Tang, A.G. Gilman, Type-specific regulation of adenylyl cyclase by G protein beta gamma subunits, Science 254 (5037) (1991) 1500–1503.
[50] R.K. Sunahara, R. Taussig, Isoforms of mammalian adenylyl cyclase: multiplicities of signaling, Mol. Interv. 2 (3) (2002) 168–184.
[51] S. Herlitze, et al., Modulation of Ca2+ channels by G-protein beta gamma subunits, Nature 380 (6571) (1996) 258–262.
[52] T. Kawano, et al., Importance of the G protein gamma subunit in activating G protein-coupled inward rectifier K(+) channels, FEBS Lett. 463 (3) (1999) 355–359.
[53] Y. Nakajima, S. Nakajima, T. Kozasa, Activation of G protein-coupled inward rectifier K+ channels in brain neurons requires association of G protein beta gamma subunits with cell membrane, FEBS Lett. 390 (2) (1996) 217–220.
[54] J.A. Pitcher, et al., Role of beta gamma subunits of G proteins in targeting the beta-adrenergic receptor kinase to membrane-bound receptors, Science 257 (5074) (1992) 1264–1267.
[55] H. Ueda, et al., Heterotrimeric G protein betagamma subunits stimulate FLJ00018, a guanine nucleotide exchange factor for Rac1 and Cdc42, J. Biol. Chem. 283 (4) (2008) 1946–1953.
[56] J. Niu, et al., G protein betagamma subunits stimulate p114RhoGEF, a guanine nucleotide exchange factor for RhoA and Rac1: regulation of cell shape and reactive oxygen species production, Circ. Res. 93 (9) (2003) 848–856.
[57] L.H. Mayeenuddin, W.E. McIntire, J.C. Garrison, Differential sensitivity of P-Rex1 to isoforms of G protein betagamma dimers, J. Biol. Chem. 281 (4) (2006) 1913–1920.
[58] K. Senarath, et al., Reversible G protein betagamma9 distribution-based assay reveals molecular underpinnings in subcellular, single-cell, and multicellular GPCR and G protein activity, Anal. Chem. 88 (23) (2016) 11450–11459.
[59] S.R. Neves, P.T. Ram, R. Iyengar, G protein pathways, Science 296 (5573) (2002) 1636–1639.
[60] M.H. Bailey, et al., Comprehensive characterization of cancer driver genes and mutations, Cell 173 (2) (2018) 371–385 (e18).
[61] L. Ding, et al., Perspective on oncogenic processes at the end of the beginning of cancer genomics, Cell 173 (2) (2018) 305–320 e10.
[62] M. Chisari, et al., G protein subunit dissociation and translocation regulate cellular response to receptor stimulation, PLoS One 4 (11) (2009) e7797.
[63] D. Kankanamge, et al., Melanopsin (Opn4) utilizes Galphai and Gbetagamma as major signal transducers, J. Cell Sci. 131 (11) (2018).
[64] S. Samaradivakara, et al., G protein gamma (Ggamma) subtype dependent targeting of GRK2 to M3 receptor by Gbetagamma, Biochem. Biophys. Res. Commun. 503 (1) (2018) 165–170.
[65] A.M. Krumins, A.G. Gilman, Targeted knockdown of G protein subunits selectively prevents receptor-mediated modulation of effectors and reveals complex changes in non-targeted signaling proteins, J. Biol. Chem. 281 (15) (2006) 10250–10262.
[66] P. Siripurapu, et al., Two independent but synchronized Gbetagamma subunit-controlled pathways are essential for trailing-edge retraction during macrophage migration, J. Biol. Chem. 292 (42) (2017) 17482–17495.
[67] A. Colaprico, et al., TCGAbiolinks: an R/Bioconductor package for integrative analysis of TCGA data, Nucleic Acids Res. 44 (8) (2016) e71.
[68] K. Wang, et al., MapSplice: accurate mapping of RNA-seq reads for splice junction discovery, Nucleic Acids Res. 38 (18) (2010) e178.
[69] M. Rahman, et al., Alternative preprocessing of RNA-sequencing data in the Cancer Genome Atlas leads to improved analysis results, Bioinformatics 31 (22) (2015) 3666–3672.
[70] B. Li, C.N. Dewey, RSEM: accurate transcript quantification from RNA-Seq data with or without a reference genome, BMC Bioinforma. 12 (1) (2011) 323.
[71] S. Mukhopadhyay, E.M. Ross, Rapid GTP binding and hydrolysis by G(q) promoted by receptor and GTPase-activating proteins, Proc. Natl. Acad. Sci. U. S. A. 96 (17) (1999) 9539–9544.
[72] P. Navaratnarajah, A. Gershenson, E.M. Ross, The binding of activated Galphaq to phospholipase C-beta exhibits anomalous affinity, J. Biol. Chem. 292 (40) (2017) 16787–16801.
[73] J. Takasaki, et al., A novel Galphaq/11-selective inhibitor, J. Biol. Chem. 279 (46) (2004) 47438–47445.
[74] D. Billups, et al., Modulation of Gq-protein-coupled inositol trisphosphate and Ca2+ signaling by the membrane potential, J. Neurosci. 26 (39) (2006) 9983–9995.
[75] J.T. Toth, et al., BRET-monitoring of the dynamic changes of inositol lipid pools in living cells reveals a PKC-dependent PtdIns4P increase upon EGF and M3 receptor activation, Biochim. Biophys. Acta 1861 (3) (2016) 177–187.
[76] A.C. Magalhaes, H. Dunn, S.S. Ferguson, Regulation of GPCR activity, trafficking and localization by GPCR-interacting proteins, Br. J. Pharmacol. 165 (6) (2012) 1717–1736.
[77] R.D. Rainbow, et al., Small-molecule G protein-coupled receptor kinase inhibitors attenuate G protein-coupled receptor kinase 2-mediated desensitization of vasoconstrictor-induced arterial contractions, Mol. Pharmacol. 94 (3) (2018) 1079–1091.
[78] T.J. Cahill 3rdet al., Distinct conformations of GPCR-beta-arrestin complexes mediate desensitization, signaling, and endocytosis, Proc. Natl. Acad. Sci. U. S. A. 114 (10) (2017) 2562–2567.
[79] V. Wolters, et al., Influence of galphaq on the dynamics of m3-acetylcholine receptor-g-protein-coupled receptor kinase 2 interaction, Mol. Pharmacol. 87 (1) (2015) 9–17.
[80] T. Eichmann, et al., The amino-terminal domain of G-protein-coupled receptor kinase 2 is a regulatory Gbeta gamma binding site, J. Biol. Chem. 278 (10) (2003) 8052–8057.
[81] M. Jafferjee, et al., GRK2 up-regulation creates a positive feedback loop for catecholamine production in chromaffin cells, Mol. Endocrinol. 30 (3) (2016) 372–381.
[82] J.-S. Lee, Exploring cancer genomic data from the cancer genome atlas project, BMB Rep. 49 (11) (2016) 607–611, https://doi.org/10.5483/BMBRep.2016.49.11.145.
[83] G. Berstein, et al., Phospholipase C-beta 1 is a GTPase-activating protein for Gq/11, its physiologic regulator, Cell 70 (3) (1992) 411–418.